sustainability

MDPI

Article

Sustainable Microbial Lead Removal Using an Upflow Anaerobic Sludge Blanket Reactor: Advancing Eco-Friendly Solutions for Heavy Metal Remediation

Bayandza M. Manzini [1], Carla Cilliers [1], Job Tatenda Tendenedzai [1], Nils H. Haneklaus [2,3,*], Evans Chirwa [1] and Hendrik G. Brink [1,*]

[1] Department of Chemical Engineering, University of Pretoria, Pretoria 0028, South Africa; u15127894@tuks.co.za (B.M.M.); u14053901@tuks.co.za (C.C.); jtendenedzai@gmail.com (J.T.T.); evans.chirwa@up.ac.za (E.C.)
[2] Transdisciplinary Laboratory Sustainable Mineral Resources, University for Continuing Education Krems, 3500 Krems, Austria
[3] Unit for Energy and Technology Systems-Nuclear Engineering, North-West University, 11 Hoffman Street, Potchefstroom 2520, South Africa
* Correspondence: nils.haneklaus@donau-uni.ac.at (N.H.H.); deon.brink@up.ac.za (H.G.B.)

Abstract: This study investigates the use of a UASB (Upflow Anaerobic Sludge Blanket) reactor operating under continuous anoxic conditions to remediate Pb(II) contamination in aqueous environments. Two experimental runs were conducted to evaluate the microbiome's performance in removing Pb(II) at varying concentrations, ranging from 80 to 2000 ppm, while monitoring nitrate and Pb(II) levels. Metabarcoding of the 16S rRNA gene was done to understand the detoxification mechanisms utilised by the microbial community in Pb(II) removal. The system demonstrated high robustness, achieving up to 99% Pb(II) removal efficiency with sufficient nutrient availability, particularly at 15 g/L yeast extract (YE), compared to lower nutrient levels of 5 g/L YE. Denitrification was identified as the dominant mechanism of detoxification, supported by additional processes such as biosorption, sulfur-reducing bacterial activity, bioprecipitation, and bioremoval. Analysis of the precipitate recovered from the reactor indicated the presence of elemental lead, PbS, and PbO, highlighting the potential for lead recovery. These findings suggest that the system not only effectively removes Pb(II) from contaminated environments but also offers a sustainable pathway for lead recovery through smelting, making it a promising circular bioremediation strategy. The results indicate that this biological approach is a viable solution for lead pollution and recovery in industrial applications.

Keywords: biosorption; denitrification; lead bioremediation; lead recovery; UASB reactor

Citation: Manzini, B.M.; Cilliers, C.; Tendenedzai, J.T.; Haneklaus, N.H.; Chirwa, E.; Brink, H.G. Sustainable Microbial Lead Removal Using an Upflow Anaerobic Sludge Blanket Reactor: Advancing Eco-Friendly Solutions for Heavy Metal Remediation. *Sustainability* **2024**, *16*, 10602. https://doi.org/10.3390/su162310602

Academic Editor: Agostina Chiavola

Received: 12 October 2024
Revised: 15 November 2024
Accepted: 29 November 2024
Published: 3 December 2024

1. Introduction

The use and availability of lead (Pb) are critical components in various technologies, industries, and other human activities. Processes like the manufacturing of storage batteries, plumbing materials, and the recycling of lead-based products increase its interaction with the environment [1]. However, one of the major drawbacks of lead use is that it ranks among the most toxic and harmful elements, making it a significant pollutant of soil, plants, and water. While lead pollution can occur naturally, it is predominantly driven by human activities [2]. Anthropogenic activities have increased Pb concentration in the environment by a 1000 times in the past 300 years [3]. Therefore, the removal and recovery of lead are critically important.

The toxicity of contamination is influenced by several factors, including the dosage (concentration), route of exposure, and the chemical species involved [4]. In this study, the focus is on Pb(II) contamination in the aquatic environment. The margins of lead toxicity

are particularly narrow due to its high potency as a pollutant. Lead contamination in water and soil can cause sub-chronic effects even at low concentrations [5], acute changes at moderately high concentrations [6], and catastrophic ecosystem damage at very high concentrations [7]. For example, concentrations of 10 ppm (10 mg/L) can disrupt endocrine activity in sensitive species, while levels above 1000 ppm can wipe out entire ecosystems [8]. The World Health Organization (WHO) sets the threshold limit for Pb(II) in drinking water at 0.05 ppm, which is also the limit for industrial wastewater according to the Environmental Protection Agency (EPA) [9]. In South Africa, the allowable limit is even stricter at 0.02 ppm [10].

The aquatic environment is particularly vulnerable to contamination because lead becomes significantly more mobile and bioavailable in its ionic form. This increases its threat to global ecosystems, including both aquatic plants and human life [11]. Key sources of this pollution include mining waste, landfill leachates, and discharges from municipal and industrial wastewater [12]. The significant signs of exposure to Pb contamination include: Central nervous system (CNS) damage in animals [13], reduced pollen production and reduced seed availability in plants/crops [14]. For human health, no safe level of lead exposure has been identified. More than 50% of inhaled lead can reach the lungs, and all ingested lead is absorbed by the digestive system [15]. Lead exposure can result in cardiovascular, gastrointestinal, neurological, haematological, and reproductive damage, making its toxicity detrimental to nearly every organ system in the human body [11].

Mitigation measures to limit and remove Pb toxicity from the environment can be categorized into conventional and bioremediation methods. Conventional treatment methods include membrane filtration, chemical precipitation, and ion exchange. Membrane filtration is advantageous due to its high efficiency and low space requirements [16]. Chemical precipitation, known for its low capital cost, and ion exchange, both exhibit good removal efficiency for heavy metals such as cadmium (Cd), lead (Pb), and arsenic (As) from water [17–19]. However, these conventional methods face challenges like non-selectivity, low efficiency, and increased waste production, underscoring the need for more cost-effective and environmentally sustainable alternatives [20].

An alternative to conventional treatment is bioremediation, which relies on enhancing the detoxification and degradation processes that microorganisms naturally employ to eliminate pollutants from the environment [21,22]. Many microorganisms possess the innate ability to degrade, transform, or chelate toxic chemicals [23]. By harnessing and accelerating these processes, environmental clean-up can be achieved without introducing additional ecological risks [24]. When microorganisms encounter heavy metals, they do not simply transfer pollutants from one medium to another, as many conventional clean-up technologies do. Instead, they degrade and transform the contaminants directly through metabolic degradation or conversion pathways [25]. Microbes can restore the environment using several mechanisms, including biosorption, complexation, precipitation, and oxidation-reduction reactions [26].

Bioremediation offers several advantages. Firstly, most of the metabolic processes involved in bioremediation occur at ambient temperatures, eliminating the need for chemical catalysts, as they are naturally catalysed by digestive enzymes [17]. Additionally, bioremediation processes are flexible, as they can be applied both in situ and ex situ to clean polluted sites. Another benefit is that microbes can be sourced from already contaminated sites, reducing the cost of purchasing feed materials for the process [26]. Lastly, the maintenance and management of these biological systems are generally less labour-intensive, as the microbes will thrive in environments that support their growth and metabolism [27]. These principles have been used in the development of several clean-up technologies and bioreactors for wastewater decontamination. Bioreactors such as: the stirred tank bioreactor for anaerobic treatment, aerobic stirred tank reactor and upflow anaerobic sludge blanket (UASB) reactor have been implemented in multiple industries to that effect [28].

The reactor used in this study was a UASB reactor, this system has been used in multiple cases of wastewater treatment and offers several benefits as a remediation solution.

This reactor has been used in the beverage, as well as pulp and paper processing industries to treat effluents [29,30]. The system can be shut down for extended periods without significant reduction in removal efficiency, the system can handle organic shock loads effectively and has low energy requirement for the treatment process [31]. These reasons along with reduced bio-waste from wastewater treatment make it an attractive option for Pb(II) removal [31].

This article evaluates a novel eco-friendly bioremediation process using a live biological system comprising a locally sourced industrial bacterial consortium and a UASB reactor for continuous Pb(II) removal from aqueous environments. The study investigated the effects of Pb(II) concentration and nutrient levels in the feed to gain deeper insights into the microbiome's behavior during the continuous removal process. The findings demonstrated a promising method for the removal and recovery of Pb(II).

Throughout the study the concentration of Pb(II) and nitrate ions in the effluent were monitored to establish the contamination limits the system can withstand. The test concentration range, 80–2000 ppm, was selected to simulate wastewater effluents from diverse sources. For instance, effluent streams from the battery industry are known to contain significant levels of lead, with concentrations often reported to be a minimum of 10 ppm [32]. In addition to this, irrigation wastewater generally falls between 0–52.4 ppm [29] and Acid Mine Drainage effluent can contain lead levels ranging from 0 to 5000 ppm [30].

A multi technique analysis was used to identify the Pb-species in the precipitate as a means to investigate the potential for Pb recovery from the system. A combination of XRD/XPS and XRF were used in that effect. Following this, genomic DNA was extracted from the samples taken throughout both runs. These samples were polymerase chain reaction (PCR) amplified using barcoded universal primer pairs which targeted the V1–V9 region of the bacterial 16S rRNA gene. This genetic analysis shed light on the changes that the microbial community underwent as a response to the changes in the reactor environment. In addition, the precipitate analysis along with metabarcoding of the 16S rRNA gene were used to link the relevant detoxification mechanisms which were expressed by the microbial community.

2. Materials and Methods

2.1. Reactor Design and Sampling

The design of the UASB reactor was adapted from the original design presented by Chimhundi et al. (2021) [33]. The modification involved introducing the feed flow from the bottom of the column. The reactor featured four potential effluent exit points along its height, with three designated sampling ports labelled 1, 2, and 3, positioned at different heights along the vertical axis. The fourth exit point served as an overflow to a waste collection point. The entire column was housed in a warm room maintained at a temperature of 30–35 °C, while the reactor feed was stored separately at 5 °C to minimize microbial growth and the risk of cross-contamination. The feed was spiked with varying Pb(II) concentrations of 80, 250, 500, 1000, and 2000 ppm, using $Pb(NO_3)_2$ as the contaminant source. The feed was supplemented with a nutrient broth containing either 5 g/L or 15 g/L of yeast extract and 1 g/L of NaCl. It was pumped at a constant flow rate of 0.86 mL/min (equivalent to 1238 mL/day), resulting in a hydraulic residence time (HRT) of 8 days. A dripper system was used to introduce the feed into the column, as visually represented in Figure 1.

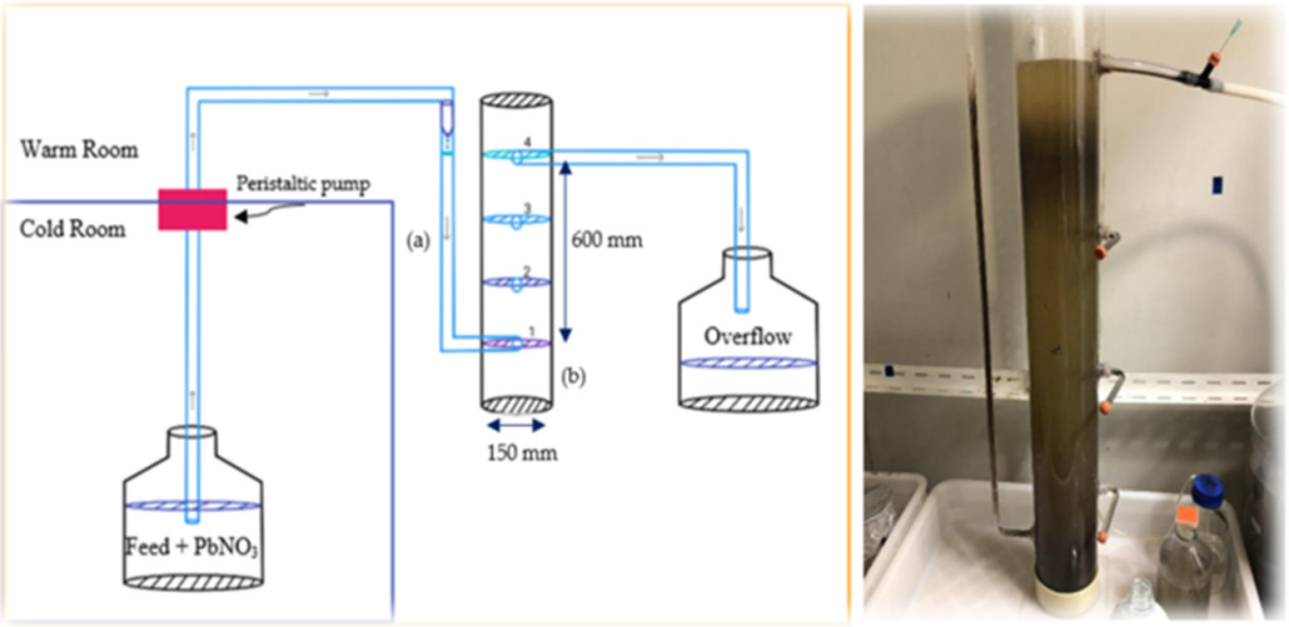

Figure 1. Upflow Anaerobic sludge blanket reactor (UASBR) column design alongside the real image. (**a**) inlet feed line (**b**) reactor column vessel.

Daily 10 mL samples were collected using a sterile syringe and needle, with the first 10 mL discarded to ensure the samples accurately represented the column contents. Prior to sampling or analysis, the reactor was primed for one month with a consistent 80 ppm Pb(II) concentration and inoculated with a microbial consortium preculture, marking the start of the official experiment. Since $PbCl_2$ tends to precipitate at lower temperatures (e.g., in the cold room), the Pb(II) concentrations in the feed were lower than expected. This variation was addressed by reporting both the theoretical (predicted) and actual measured Pb(II) concentrations in the feed stream.

The experiment involved two experimental runs: Run 1, lasting 20 days, and Run 2, lasting 30 days. In Run 1, the reactor was charged with Pb(II) concentrations of 80, 250, 500, 1000, and 2000 ppm, while Run 2 was loaded with 80, 250, 500, and 1000 ppm Pb(II). The nutrition dosing schedules for both runs are presented in Tables 1 and 2, respectively.

Table 1. Run 1 Experimental timeframe and dosing schedule.

[Pb(II)]	80 ppm	500 ppm	250 ppm	250 ppm	1000 ppm	2000 ppm
Nutrient concentration	15 g/L YE 1 g/L NaCl	5 g/L YE 1 g/L NaCl	5 g/L YE 1 g/L NaCl	15 g/L YE 1 g/L NaCl	15 g/L YE 1 g/L NaCl	15 g/L YE 1 g/L NaCl
Days	0–3	4–9	10–13	14–16	17–18	19–20

Table 2. Run 2 Experimental timeframe and dosing schedule.

[Pb(II)]	80 ppm	500 ppm	250 ppm	250 ppm	80 ppm	250 ppm	500 ppm	1000 ppm
Nutrient concentration	15 g/L YE 1 g/L NaCl	5 g/L YE 1 g/L NaCl	5 g/L YE 1 g/L NaCl	15 g/L YE 1 g/L NaCl	15 g/L YE 1 g/L NaCl	15 g/L YE 1 g/L NaCl	15 g/L YE 1 g/L NaCl	15 g/L YE 1 g/L NaCl
Days	0–3	3–10	10–17	17–21	21–24	24–26	26–28	28–30

To observe the reduction in lead concentration, it was essential to note the initial concentrations and track the changes over time during both experimental runs. Due to the precipitation of lead in the feed reservoir, the actual initial lead concentrations were lower than the predicted values. These true initial concentrations are reported in the tables below for both runs. Additionally, nitrate concentrations were measured from the initial feed and monitored throughout the course of the experiments. The influent ion concentrations for both lead and nitrate are presented in Tables 3 and 4 below.

Table 3. Initial UASB reactor feed Pb(II) and Nitrate Concentrations for Run 1.

Anticipated Initial Pb(II) Concentration (ppm)	True Inlet Pb(II) Concentration (ppm)	Inlet Nitrate Concentration (ppm)
80 ppm (A)	72.4	76.3
500 ppm (B)	192	174
250 ppm (C)	72.2	118
250 ppm (D)	210	182
1000 ppm (E)	529	210
2000 ppm (F)	860	1148

Table 4. Initial UASB Reactor feed Pb(II) and Nitrate Concentrations for Run 2.

Anticipated Initial Pb(II) Concentration (ppm)	True Inlet Pb(II) Concentration (ppm)	Inlet Nitrate Concentration (ppm)
80 ppm (A)	69.6	42.7
500 ppm (B)	211	327
250 ppm (C)	135	117
250 ppm (D)	135	117
80 ppm (E)	69.6	42.7
250 ppm (F)	135	117
500 ppm (G)	211	327
1000 ppm (H)	357	681

These tables provide a detailed comparison between the predicted and actual concentrations, allowing for a better understanding of the lead reduction process during the UASB reactor operation in both experimental runs.

2.2. Microbial Preparation

The Pb(II)-resistant microbial consortium was sourced from a borehole at an automotive battery recycling facility in Gauteng, South Africa [8]. To prepare the initial inoculum, 1 g of Pb(II)-contaminated soil was introduced into LB broth supplemented with 80 ppm Pb(II) in a 100 mL anaerobic serum bottle, followed by incubation at 32 °C and 120 rpm for 24 h. The inoculum was cryogenically stored with glycerol at a final ratio of 20% v/v at −77 °C. Precultures were prepared from the stored inoculum by inoculating 100 mL anaerobic serum bottles spiked with approximately 80, 250, 500, and 1000 ppm Pb(II) respectively. The serum bottles were sealed and incubated at 30 °C and 120 rpm until precipitation was visible. The new precultures were again cryogenically stored for direct inoculation of the experiments [17].

2.3. Materials

The reactor feed was spiked with a lead stock solution prepared with $Pb(NO_3)_2$ (Merck, Kennelworth, NJ, USA), the growth medium contained either 5 or 15 g/L of Yeast extract (YE) and 1 g/L NaCl. DNA extractions were carried out using the DNeasy® Powerlyzer® PowerSoil® Kit and reagents from QIAGEN (Johanneburg, South Africa). The Qubit analysis was done using Invitrogen Qubit™ dsDNA BR Assay kit and the dsDNA HS Assay kit (Johannesburg, South Africa). Gel visualising was done using gel prepared with

Agarose powder, SYBR Safe, DNA Gel Strain (10,000× Concentrate in DMSO) and 50× Tris-Borate-EDTA (TBE) solution. Gel loading dye was used in loading the wells in the gel.

2.4. Ion Measurements

Pb(II) and NO_3^- ions were analyzed using Ion Chromatography (IC) with a 940 Professional IC Vario system (Metrohm, Herisau, Switzerland). Separation was performed using a Metrosep C 6–250/4.0 column and an eluent of 8 mM oxalic acid (Metrohm, Herisau, Switzerland). Since Pb(II), a transition metal, is not effectively detected via conductivity, UV-Vis detection (Metrohm, Herisau, Switzerland) at 520 nm was employed. This was facilitated by a post-column reaction using PAR (pyridylazoresorcinol, Thermo Fisher Scientific, Waltham, MA, USA) in combination with HNO_3 and 25% NH_4OH (both sourced from Glassworld, Robertville, Johannesburg, South Africa) [34]. Pb(II) ions were also measured with the use of an atomic absorption spectrometer (Perkin Elmer AAnalyst 400, Waltham, MA, USA) equipped with a Pb Lumina hollow cathode lamp (Perkin Elmer AAnalyst 400, Waltham, MA, USA). All measurements were done in triplicate and average concentration was reported.

2.5. Precipitate Identification

Samples for precipitate analysis were collected during Run 1 of the study. The contents of the reactor were collected at concentrations of 80, 250, 1000 and 2000 ppm. The effluent was centrifuged at 9000 rpm for 15 min (at 25 °C), the pellet was removed and dried in an oven set to 35 °C for 48 h. A pestle and mortar were used to pulverise the samples to sub-80 µm particle size prior to analysis. Precipitate identity was confirmed with X-Ray Diffraction (XRD) with an X-ray diffractometer and the XRD-profiles were analysed using the X-ray diffraction software package Match!3 (Crystal Impact GbR, Bonn, Germany) [35]. To support the results obtained from XRD a subsequent XPS analysis was ordered. The XPS analysis was used to determine the chemical state of the elements and composition of materials in the reactor precipitate [36].

2.6. DNA Extractions

The DNA extraction methods for both runs were conducted according to the guidelines on the extraction kits. The extraction method for Run 1 is available in the DNeasy® Powerlyzer® PowerSoil® Kit manual [37]. All solutions needed for the extraction process are provided in the kit. A total of 48 DNA extractions were completed with this kit. The tubes containing extracted DNA were sealed and stored at −80 °C. Samples from Run 2 were extracted at Inqaba Biotechnical Industries. In this case, the genomic DNA was extracted using ZymoBIOMICS DNA MiniPrep kit (Zymo Research) following the manufacturer's protocol [38].

After DNA extractions were completed, Qubit assays were done to measure the concentration of DNA in the samples. The Qubit assays were prepared using Invitrogen Assay kits. The first 20 samples were checked using dsDNA (Double stranded DNA) HS (High sensitivity) Qubit Assay kit. The following 28 samples were performed using the dsDNA BR (Broad range) Assay kit was used due to limitations in resources. Samples were prepared by pipetting 10 µL of the extracted DNA and adding 190 µL of the working solution (BR/HS) reagent in a Qubit Assay tube. The assay tubes were vortexed for 3–5 s while ensuring that bubbles did not form in the tubes. The tubes were then allowed to incubate at room temperature for 2 min and then analysed using the Qubit 4 fluorometer. The qubit assay is used as a measure of assessing the conentration of the DNA in the samples after extraction [39]. This analysis was done on samples from Run 1 only due to limitations in resources.

From the Qubit analysis, all samples from Run 1 which passed the minimum concentration acceptable for gel loading were prepared for visualisation. A baseline of 0.7 ng/µL was set in this case. The samples were loading using agarose gel electrophoresis. This procedure may be used as a method to separate, identify and purify the nucleic acids

in the sample from any possible contaminants which may have been picked up during extraction procedures. The procedure has been used extensively in the field of virology and has shown success in genomic detection and strain characterization [40]. The procedure followed in gel preparation was based on work previously covered by Armstrong & Schulz (2015). The DNA marker used in this process was bromophenol blue and the gel was placed in electrophoresis tank. Once the marker had moved sufficiently (about two thirds from the top of the tray) after running it in the tank at 150 volts, the gel was removed from the tank and visualised on a UV transilluminator [41]. The 16S rRNA gene metabarcoding for both Runs was sent to Inqaba Biotechnical Industries. Inqaba made use of the PacBio (Pacific Biosciences) Revio system for this procedure. This system targets the relevant individual genes or small gene panels using a PCR-based approach [42]. The genomic DNA samples were polymerase chain reaction (PCR) amplified using barcoded universal primer pair 27F and 1492R (12× 27F barcoded primers and 8× 1492R barcoded primers), targeting the V1–V9 region of the bacterial 16S rRNA gene [43]. The resulting barcoded amplicons were quantified individually and then pooled. An equimolar pooling step was performed, followed by purification using AMPure PB bead-based technology. The PacBio SMRTbell library was subsequently prepared from the pooled amplicons according to the manufacturer's protocol, starting from step 3: Pool and Cleanup [43].

3. Results and Discussions

3.1. Lead Removal

In the following figures, the measured Pb(II) concentrations at different sampling points are presented. During the first run, samples were collected from all three designated sampling points, while in the second run, only two sampling points were utilized. Tables 3 and 4 correspond to Figures 2 and 3, respectively, and provide a key to match the inlet feed concentrations with the relevant sections in the figures. Tables 1 and 2 relate to the nutritional dosing schedule for Figures 1 and 2 respectively. This organization helps clarify the relationship between the Pb(II) concentration in the feed and the observed reductions at each sample point, offering insights into the effectiveness of the UASB reactor across both experimental runs.

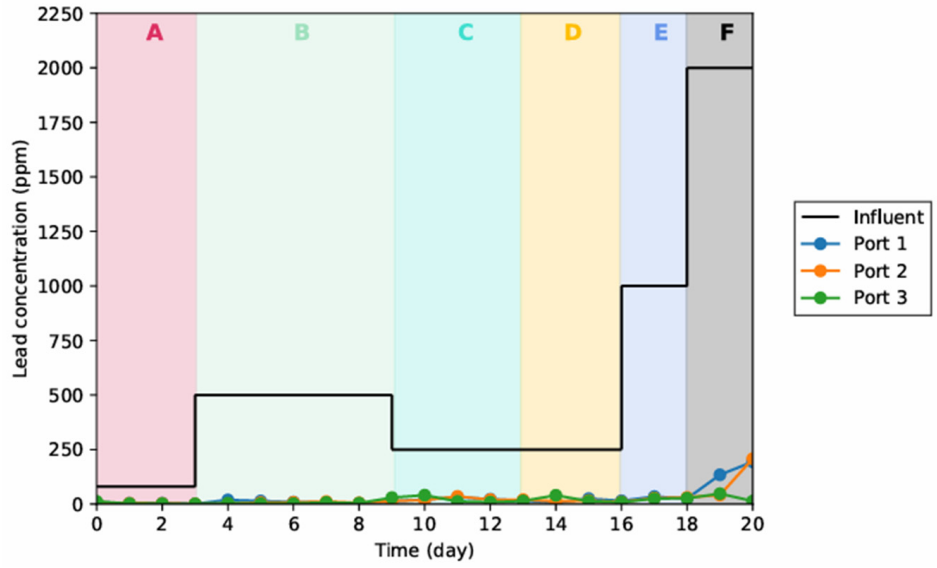

Figure 2. Pb(II) concentrations measured at ports 1, 2 and 3 respectively in Run 1. The letters (A–F) at the top of the graph represent the different influent conditions mentioned in Table 3, i.e., Section A—80 ppm feed.

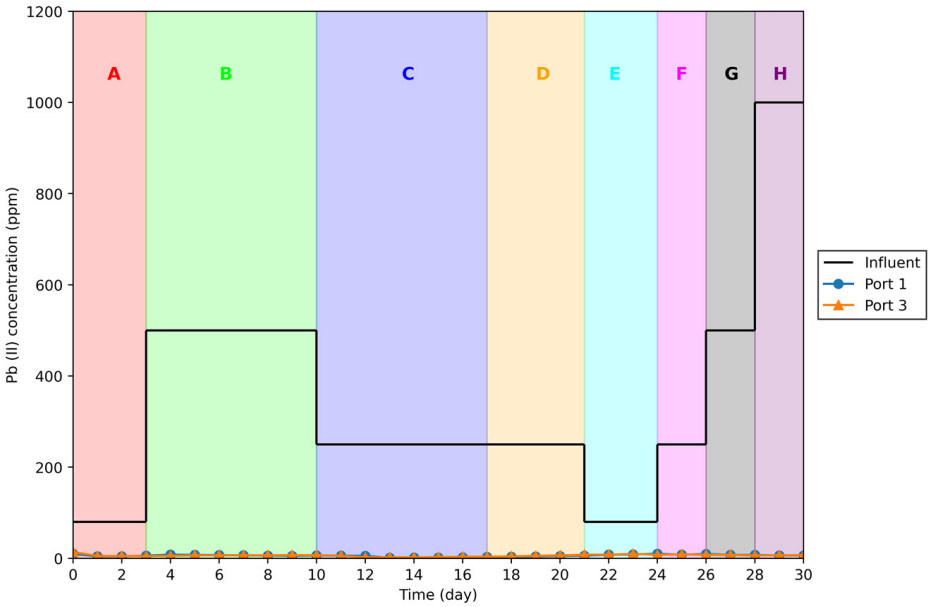

Figure 3. Pb(II) concentrations measured at ports 1 and 3 respectively in Run 2. The letters (A–H) at the top of the graph represent the different influent conditions mentioned in Table 4, i.e., Section A—80 ppm feed.

The figures above demonstrate that biological remediation of Pb from aqueous environments is feasible using the bacterial consortium in the UASB reactor. Near-complete removal of lead was achieved across all feed concentrations in both experimental runs. Notably, during the second run, complete lead removal was observed for all concentrations without any spikes in effluent concentrations. In contrast, the first run exhibited a breakthrough of Pb around day 19, coinciding with the highest influent Pb concentration. Run 1 resulted in effluent concentration variation between 0 and 194.38 ppm. This effluent discharge did not meet the effluent discharge limit on enough occasions and it would require a further treatment stage to meet discharge limits. During Run 2, the effluent concentration was maintained between 0–4.15 ppm. This indicated a significant improvement in effluent quality from the system over this extended operating period. In terms of removal efficiency which was observed over the two runs, it was 92% in Run 1 and it was 96% in Run 2. The results from both runs confirmed that complete lead removal could be achieved at all sampling points. There concentration profiles for each of the sample points were also quite similar. In some areas the measured data intersects as shown in the line graphs above. This is an indication that there were no "dead zones" in the reactor where microbes were ineffective in removing lead.

It can be noted that higher feed concentrations might reduce lead removal efficiency, as observed in the first run. This effect was more pronounced in the lower sampling points, with spikes recorded in ports 1 and 2. During both runs, the highest lead concentrations were measured at port 3 for feed concentrations up to 1000 ppm. The elevated Pb levels in samples from port 3 are likely due to secondary release of Pb(II), particularly if significant amounts of lead were absorbed onto the biomass surfaces. Despite this, the system proved to be robust in managing high lead concentrations, as long as the nutrient requirements for the bacterial consortium were met.

Nutrient availability had a notable impact on Pb removal efficiency. A previous study by the authors on the same microbial consortium indicated that lead removal was less efficient when 5 g/L of yeast extract (YE) was used compared to 15 g/L YE [44]. This outcome is linked to the metabolic activity of the microbiome, where an increase in Pb(II) concentration in the effluent was associated with decreased microbial metabolic activity.

Significant precipitate formation was also observed in the reactor throughout both experimental runs, suggesting that bioprecipitation was a key microbial detoxification

mechanism in the system. This, along with other mechanisms such as immobilization or mobilization of metal ions [45], aided the microbiome in effectively removing contaminants. Other Pb removal mechanisms identified in the system include denitrification, biosorption, sulfur-reducing bacteria activity, and bioprecipitation [44]. Precipitate formation presents an additional advantage, as once the metal ions are precipitated into insoluble compounds, physical separation techniques like filtration can be employed as a final step to remove Pb from the water effectively.

Run 2 was the most effective experimental run overall. The extended number of days of continuous operation did not result in significantly reduced efficiency. The system also showed resistance to contaminant loading, with consistent nutritional availability there weren't any Pb-concentration spikes during this Run. Based on these above observations the system would need to be coupled with a further refining stage to reach surface water quality discharge or drinking water standards.

Furthermore, the measurements in Run 1 also included pH measurements. The pH measurements across all concentration ranges showed that the effluent was maintained between 6.29–6.91. The pH range of the effluent shows promising results. The World Health Organization (WHO) recommends that drinking water should have a pH between 6.5 and 8.5 [46]. The SANS 241 standards for South African drinking water stipulate a pH range of 5 to 9.7 at 25 °C [47]. Based on these standards, the effluent falls within the desired pH range following biological treatment

3.2. Precipitate Identification Discussion

During Run 1, precipitates from the column were collected for analysis, as limitations in resources allowed precipitate identification from only one run. Figure A1 present the X-ray diffraction (XRD) profiles obtained from the analysis of these precipitates. The figures reveal that the dominant species identified was Galena (PbS). This aligns with observations from a previous study, where the presence of precipitates was correlated with lead concentrations in the effluent [44]. In this study, the precipitate was washed out of the reactor through port 4, contributing to elevated Pb concentrations measured at port 3. The identification of these Pb species in the precipitate suggests that continuous bioremediation can serve as a viable method for lead recovery.

The significance of lead recovery lies in the fact that global lead depletion is estimated at a rate of 5 Mt/year, with reserves standing at 85 Mt. Based on this rate, lead reserves are projected to be depleted within the next 15–17 years [33]. Current recovery processes are disadvantageous, as they generate large volumes of toxic waste that require hazardous disposal methods and are costly [33]. The ability of bioremediation to recover lead while minimizing waste production positions it as a more sustainable and cost-effective alternative to conventional recovery processes.

After XRD characterization, the precipitate samples were further analysed using X-ray Photoelectron Spectroscopy (XPS). The XPS profiles (Figure 3), along with the identified species in the samples, are detailed below.

The XPS results confirm the presence of PbS in the precipitate across all four tested concentrations. Additionally, elemental lead (Pb^0) and lead oxide (PbO) were also detected. The presence of PbO is likely due to the oxidation of elemental lead, serving as an indicator of elemental Pb within the sample. Figure 4 displays the XPS profiles corresponding to Pb(II) loadings of 80, 250, 1000, and 2000 ppm, highlighting the variations in lead species across the different concentrations.

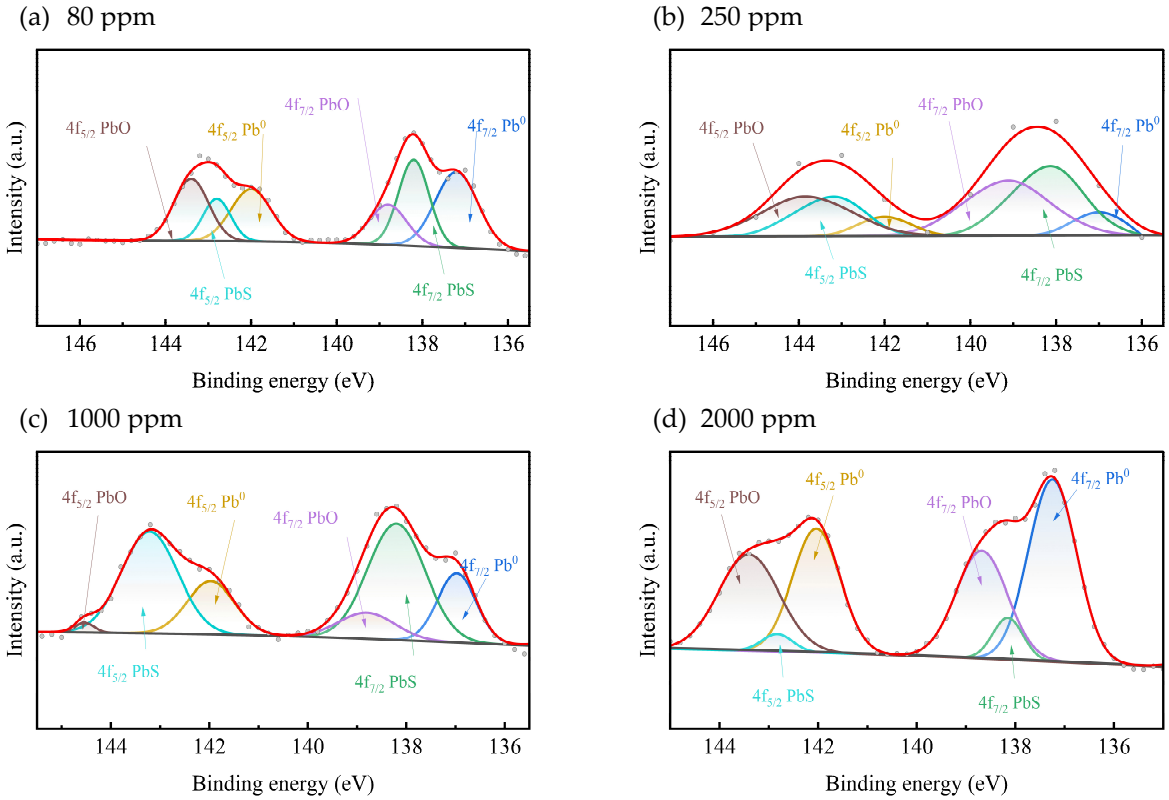

Figure 4. The XPS profiles of the precipitate obtained at the feed concentrations.

This multi-technique analysis strengthens the evidence of Pb recovery in the form of PbS, while also revealing trace amounts of elemental lead and lead oxide, providing a comprehensive understanding of the lead species present in the precipitate.

The microbial production of lead (Pb) precipitate from Pb(II) under anaerobic conditions is linked to a combination of oxidation-reduction mechanisms and sulfide liberation through the catabolism of sulfur-containing amino acids, such as cysteine and methionine [17,48]. In this process, Pb(II) acts as an electron acceptor across all concentration ranges. During the catabolism of carbon sources, CO_2 is produced, releasing electrons that reduce Pb(II) to elemental Pb, forming Pb-precipitate [17]. Similarly, the metabolism of sulfur-containing amino acids can result in the intracellular release of sulfides, which can precipitate as PbS upon interacting with Pb(II) ions in solution [17].

The presence of PbO in the precipitate is unlikely due to the oxidation of PbS, as temperatures exceeding 800 °C would be required for complete oxidation to occur. Instead, PbO and PbS are likely formed through independent pathways. It is more plausible that elemental Pb was exposed to oxidizing conditions during sample preparation for XRD/XPS, leading to its oxidation to PbO [17]. Table 5 provides details on the quantities of each Pb species in the precipitate, further elucidating the distribution of lead compounds formed in the system.

Table 5. The species and content breakdown of components in the precipitate showing PbS, PbO and Pb^0.

Feed Concentration (ppm)	Pb (%)	PbS (%)	PbO (%)
80	41.7	29.7	28.6
250	6.9	44.9	48.2
1000	27	64.4	8.6
2000	52.7	6.5	40.8

Further research is necessary to quantify the potential returns from the remediation process. However, these results suggest a promising pathway for lead recovery from processing plants and mine tailings' waste streams. The precipitate recovered, which contains significant amounts of PbS, can be recycled alongside Galena ores in lead-smelting processes. This approach offers an opportunity for sustainable lead recovery while reducing waste and mitigating environmental contamination.

3.3. Genetic Analysis

To gain genetic insights into the microbiome responsible for lead (Pb) remediation, samples were collected throughout the first and second experimental runs, covering Pb concentrations ranging from 80 to 2000 ppm. The samples were labelled A1-18 for Run 1 and B1-6 for Run 2, corresponding to Pb and yeast extract (YE) feed concentrations as outlined in Table 6. These intact samples provided invaluable insights into the microbial communities involved in Pb detoxification and bioprecipitation within the Upflow Anaerobic Sludge Blanket (UASB) reactor system.

Table 6. Sample ID and feed concentrations for genomic study. Samples were labelled A1-18 for Run 1 and B1-6 for Run 2. The table also describes the days (time period) when the samples were obtained i.e., Day 1-5 of Run 1 or Run 2.

Sample ID	Time Period (Days)	Pb-Feed Concentration (ppm)	Nutrient Concentration (g/L YE)
A1-6	0–8	80	15
A7-9	4–9	500	5
A10-12	10–13	250	5
A13-14	13–16	250	15
A15-16	17–18	1000	15
A17-18	19–20	2000	5
B1	0–3	80	5
B2	24–26	250	15
B3	21–24	80	15
B4	26–28	250	15
B5	28–30	500	15
B6	28–30	500	15

From the 16S rRNA sequencing results, a comparison was made between assigned and unassigned DNA across all samples at the first taxonomic level. Most of the DNA was assigned to known reference populations, with unassigned sequences ranging between 7% and 12% across different concentration ranges in Run 1, all DNA was assigned to existing reference populations in Run 2.The presence of unassigned sequences is particularly interesting, as they may represent novel microbial species not yet catalogued in existing reference databases [49]. This suggests that novel, previously undetected strains could be contributing to Pb remediation in the system.

From the analysis of the assigned genomic DNA, several microbial species were identified, each displaying mechanisms potentially linked to lead (Pb) removal and precipitate formation observed during the experiment. Among the identified microbial species from the assigned DNA, several genera were observed that likely play key roles in Pb removal, biosorption, and bioprecipitation. These species include those with mechanisms directly linked to Pb resistance and detoxification processes. The microbiome study revealed a strong presence of several key bacterial populations, including *Proteobacteria*, *Bacilli*, *Clostridium*, *Pseudomonas*, and sulphur-reducing bacteria across all concentration ranges. Since *Proteobacteria* and *Pseudomonas* are closely related, their abundance in this environment was expected.

Figure 5 illustrates the primary genera identified across the samples, while Table 7 summarizes the known resistances and potential roles of these genera in lead detoxification.

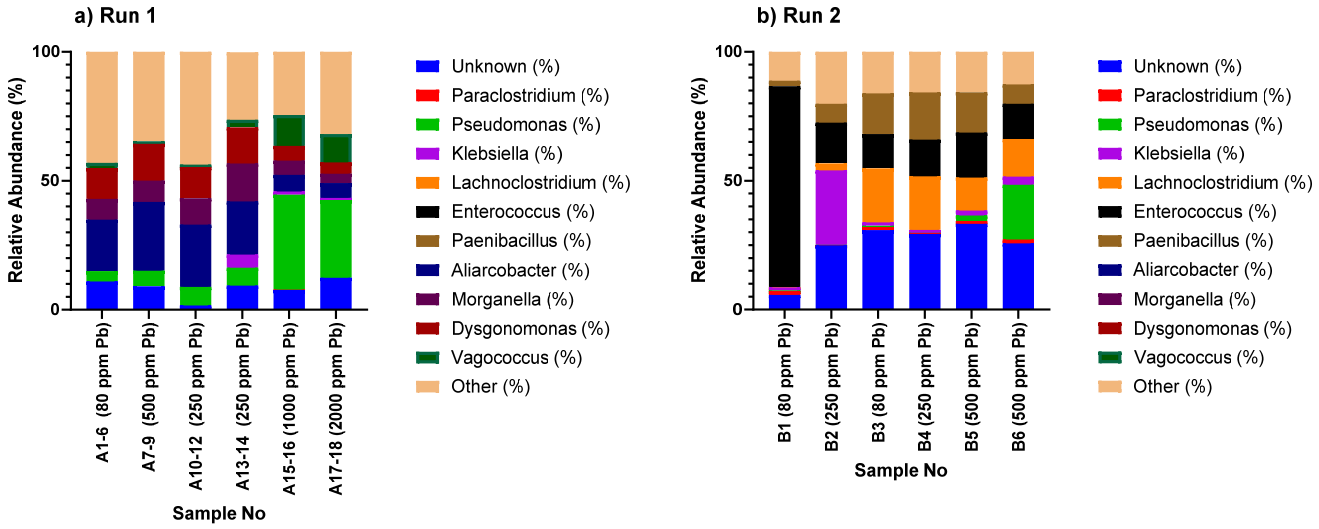

Figure 5. Identified microbial species across all concentration ranges.

It should be noted that the classifications were all done on a genus taxonomic level. In a future study it would be beneficial to go into key species identification to provide further clarity into the microbial consortium. A BLAST analysis would also be beneficial for the study to gain statistical insights of the species. For the purposes of this study, only comparisons between the genera of the two experimental runs were made. Furthermore, the results of the analysis are presented in the form of stacked bar charts which represent the relative average abundance (%) of genera in each sample. This approach has been used before in other studies for the purposes of comparing biomes from different environmental conditions [50,51]. These bar charts are displayed in Figure 5.

In Run 1, across Pb concentrations ranging from 80 ppm to 2000 ppm, *Pseudomonas* showed varying levels of abundance influenced by Pb(II) concentrations and nutrient availability. This was the case regarding all the other genera which were observed as well. The abundance of *Pseudomonas* in Run 1 was around 5% at 80 ppm and 10% at 500 ppm, indicating that while it contributed to Pb remediation, it was not the dominant player under these conditions. This abundance decreased to below 10% at 250 ppm, this decrease coincided with 5 g/L YE and it was noted that the population increased when the nutrients were increased to 15 g/L. The *Pseudomonas* were more abundant at 1000–2000 ppm, it was observed that this genus accounted for almost 30% of the microbiome under these operating conditions. In Run 2 *Pseudomonas* were not observed at lower Pb(II) concentrations. However, they accounted for almost 20–25% of the microbiome at 500 ppm. This genus's known capabilities in biosorption, exopolysaccharide production, and anaerobic denitrification [52]. This likely contributed to its increased role in Run 1, where more challenging environmental conditions demanded robust detoxification mechanisms. This was observed again in Run 2 when their population increased at 500 ppm.

Lachnoclostridium, a Gram-positive obligate anaerobe, exhibited a more stable presence across in Run 2. In Run 1 it was hardly observed, abundance was recorded between 0–5% across all concentration ranges. Even the changes made with respect to nutrient concentration did not provide any changes in its abundance during Run 1. However, in Run 2 its population varied with each successive increase of Pb(II) and each variation of the nutrient concentration. At 80 ppm with 5 g/L YE this genus was below 5%. The response to increasing influent concentration to 250 ppm Pb(II) and 15 g/L resulted in the genus' abundance increasing above 5%. Between 80–250 ppm (with 15 g/L YE) it accounted for nearly 22% of the microbiome. This suggests that its anaerobic metabolism and Pb resistance mechanisms became more favourable under these conditions of metal stress in Run 2. The genus relative abundance then decreased again to 10% at 500 ppm (15 g/L

YE). Certain *Lachnoclostridium* strains are known to be Pb-resistant and have demonstrated bioremoval capabilities in previous cases [53].

Klebsiella, a Gram-negative bacterium known for its role in denitrification and metal resistance, was present at low levels in Run 1 but saw a significant increase in abundance in Run 2. The only indication of its presence in Run 1 was between 250–2000 ppm with 15 g/L YE. What was observed is that this genus only accounted for roughly 5% of the microbiome at 250 ppm but was reduced to between 1–3% above this concentration range. These observations indicate that the role of *Klebsiella* strains was diminished with increases in Pb(II) concentrations during Run 1, in Run 2 similar observations were made regarding the genus. Its highest presence was at Pb concentrations of 250 ppm (close to 25% of the microbiome) suggesting that this genus played a greater role in Pb detoxification under these conditions. At 500–2000 ppm (in both experimental runs) the relative abundance of this strain was between 1–5%. *Klebsiella* strains contribute to nitrification and denitrification processes that likely supported overall system stability. These gram-negative strains have been previously observed in Pb-contaminated environments, such as in a microbial community from a Pb-Zn mine in Iran [54]. These strains have also exhibited biosorption and anaerobic denitrification mechanisms for detoxifying heavy metals [55].

Paraclostridium, another Gram-positive anaerobic bacterium, was hardly detected across the test concentration range in Run 1, but had a sustained presence in Run 2 at all Pb(II) concentrations. This genus accounted for 1–2% of the microbiome in Run 2 and did not appear to be particularly affected by influent conditions. However, it was observed that at higher Pb(II) concentrations in Run 2 the genus began to play less of a role in detoxification. *Paraclostridium* strains express Pb resistance and removal through sulphate reduction detoxification mechanisms [55,56].

Enterococcus strains were also detected in both experimental runs. In Run 1, the abundance of *Enterococcus* was nearly undetectable throughout all concentration ranges. In Run 2, the results showed that this genus was most abundant at 80 ppm coupled with 5 g/L YE. At these operating conditions the genus accounted for as much as 80% of the microbiome. This reduced gradually as the experimental run progressed, irrespective to changes in Pb(II) and yeast extract concentrations. All other test concentrations in this Run had relative abundance measurements between 10–15% for this genus. For *Enterococcus* bacteria, particularly *Enterococcus faecium*, resistance to heavy metals has been documented, with strains countering cadmium (Cd) and copper (Cu) toxicity. A strain of this bacteria from Italy also demonstrated resistance to Cu, Pb, nickel (Ni), and zinc (Zn) [57]. These findings suggest that the microbiome identified in this study has significant potential for heavy metal detoxification, particularly in Pb-contaminated environments.

Paenibacillus, a Gram-positive bacterium known for its biosorption and bioflocculation capabilities was also observed to be a part of the Pb(II) removing microbiome. Its detection was more frequent and the relative abundance was higher in Run 2. During this run it was first observed that the relative abundance was approximately 2% at 80 ppm and it increased to 10% at 250 ppm under constant nutrition availability (5 g/L YE) further emphasising the genus' resistance to the contaminant. When the nutrient availability was increased (15 g/L) there were noticeable changes in the measurements. Between 80–250 ppm the strains were enriched, the abundance increased from 10% at the previous stage to approximately 17–19%. It was maintained in this range up to 500 ppm where a slight decrease in abundance was noted. This genus's ability to stabilize Pb contaminants through bioflocculation [3] likely contributed to its success in the more challenging environmental conditions present in Run 2. These strains also exhibit surface biosorption capabilities, employing processes such as chelation, ion exchange, adsorption, and diffusion through cell walls and membranes to facilitate the biosorption of metal ions [3]. Additionally, biosorption and bioflocculation play crucial roles during the detoxification stage and contribute to the formation of the precipitate, aiding in lead immobilization and removal from the system.

By contrast, *Aliarcobacter* [58,59], a Gram-negative microaerophilic bacterium, was more prominent in Run 1, particularly at lower Pb concentrations (500 ppm and below).

However, its presence declined sharply in Run 2, suggesting that the microaerophilic conditions it favours were no longer dominant in Run 2. In Run 2 this genus was hardly detected as opposed to Run 1 when relative abundance reached a maximum value of 38% between 80–250 ppm. This is a strain that is commonly found in the gut microbiota of farm animals and is a foodborne pathogen. It is highly mobile in water and its detection may be linked to the origin of the microbial consortium [59]. Its antimicrobial resistance was likely to be the cause of its survival in the Pb(II) contaminated environment, but no solid Pb(II) removal mechanisms associated with this genus have been established yet [58].

Morganella is a Gram-negative facultative anaerobe. It was mostly present in Run 1, the highest relative abundance was obtained at 250 ppm (15 g/L YE). The genus was positively affected by increases in yeast extract however, the limits of resistance were decreased at 1000–2000 ppm. At its highest, the relative abundance of this genus was approximately 15%, and this gradually decreased to 2–5% at 2000 ppm. Its ability to resist metal stress [60,61] likely made it a key player in Pb remediation as the experimental conditions became more challenging. In Run 2, this genus played less of an important role in Pb(II) removal and its detection was below 5% across all concentration ranges.

Table 7. Main bacteria identified in the microbiome study.

Genus	Gram-Positive/Negative	Shape	Oxygen Requirements	Known Resistance and Mechanisms	References
Pseudomonas	Gram-negative	Rod	Oxidase Negative	Known Pb resistance. Biosorption capabilities, Exopolysaccharide production, biosorption, anaerobic denitrification	[52,62–64]
Lachnoclostridium	Gram-positive	Rod	Obligate Anaerobe	Known Pb resistance and removal.	[53,65]
Klebsiella	Gram-negative	Rod	Oxidase negative	Known Pb resistance and removal. Nitrification, Denitrification	[55,66,67]
Paraclostridium	Gram-positive	Rod	Obligate Anaerobe	Known Pb resistance and removal. Sulphate reduction	[55,56,68]
Enterococcus	Gram-positive	Cocci	Anaerobic	Known Pb resistance and removal. Denitrification	[57,69–71]
Paenibacillus	Gram-positive	Rod	Oxidase Negative	Known Pb resistance and removal. Biosorption and bioflocculation.	[72,73]

Table 7. *Cont.*

Genus	Gram-Positive/Negative	Shape	Oxygen Requirements	Known Resistance and Mechanisms	References
Aliarcobacter	Gram-negative	Spiral	Microaerophilic	Possible antimicrobial resistance, found in farm animals and water.	[58,59]
Morganella	Gram-negative	Rod	Facultative Anaerobe	Known metal resistance.	[60,61]
Dysgonomonas	Gram-negative	Rod	Obligate Anaerobe	Known antibiotic resistance.	[74,75]
Vagococcus	Gram-positive	Cocci	Facultative Anaerobe	Known metal and antibiotic resistance.	[76,77]

Dysgonomonas, another Gram-negative anaerobe, were more abundant in Run 1, particularly in the range between 80–500 ppm. However, the Pb(II) resistance decreased significantly above 500 ppm. In Run 2, the genus hardly appeared in the samples indicating that the microbiome was using other microbes to facilitate Pb(II) removal in the same range from 80–500 ppm. Throughout Run 1, this genus' relative abundance was between 5–20% across all concentrations and the highest reading was obtained at 250 ppm (15 g/L YE). It should be noted that this genus did not seem to be particularly dependent on nutrient availability. There were no significant increases in relative abundance which can be linked directly to nutrient availability in the feed. However, the increase in Pb(II) was the pivotal variable change which resulted in decreased abundance from approximately 20% at the peak (250 ppm) to approximately 4–5% above 1000 ppm. This genus has known resistance to antibiotics and its anaerobic metabolism [74,75] likely allowed it to thrive in the high-Pb, low-oxygen conditions of Run 1.

Finally, *Vagococcus*, a Gram-positive facultative anaerobe increased in abundance at higher Pb concentrations in Run 1. This genus was dominant at 100–2000 ppm in Run 1. Its relative abundance appears to have been dependent on nutrient concentration. This is because, between 80–500 ppm at 5 g/L YE the relative abundance was in the range of 3–5%. However, this increased to significantly when 15 g/L YE was fed. The abundance peaked at roughly 15% when 1000 ppm and only decreased by 1–2% at 2000 ppm. The implication of this observation was that the impact of nutrient concentration was more significant than that of Pb(II) concentration. In Run 2, this genus was hardly detected, its role in Pb(II) removal was comparatively less significant in this case. Its resistance to metals and antibiotics [76,77] likely made it an important component of the microbial community responsible for Pb detoxification, particularly as metal stress increased in Run 1.

Overall, the changes observed between Runs 1 and 2, particularly in relation to Pb concentration, reveal a clear adaptation of the microbial community. The variation in relative abundance of metal-resistant and anaerobic genera such as *Pseudomonas*, *Morganella*, *Vagococcus*, and *Paenibacillus* reflected the increasing demand for robust metal detoxification mechanisms as Pb concentrations rose. Meanwhile, genera like *Aliarcobacter*, which thrived under the operating conditions in Run 1, saw a decline in abundance in Run 2. The observations made in this analysis confirmed that the changes in Pb(II) and nutrient levels resulted in several changes in the microbial community. These changes enhanced the microbiome's capability to maintain its Pb-remediation under more challenging environmental conditions. There was also a decrease in the abundance of several microbes which were identified in Run 1. Run 1 had the most diverse population of bacteria, there were multiple identified strains, even some which still need research to conclude if they play a role in Pb(II) remediation. An example of one of these strains is *Campylobacterales*. This strain is a gram-negative bacterium which falls under the *Proteobacteria* phylum. Previous

studies have shown that these bacteria play a role in sulphate reduction under euxinic conditions [78]. Euxinic conditions occur when water is both anoxic and sulfidic [79], similar to the conditions found in the bioreactor.

3.4. Nitrate Tracing

The microbiome population demonstrates a significant presence of microbes that contribute to denitrification as a detoxification mechanism. This was observed in both experimental runs, where nitrate ion measurements were conducted to track the changes in nitrate concentrations throughout the system. The profiles of these concentration measurements can be seen in Figures 6 and 7, illustrating the role of denitrification in the overall Pb detoxification process. This mechanism likely played an essential part in reducing nitrate levels and aiding in the microbial community's heavy metal remediation efforts.

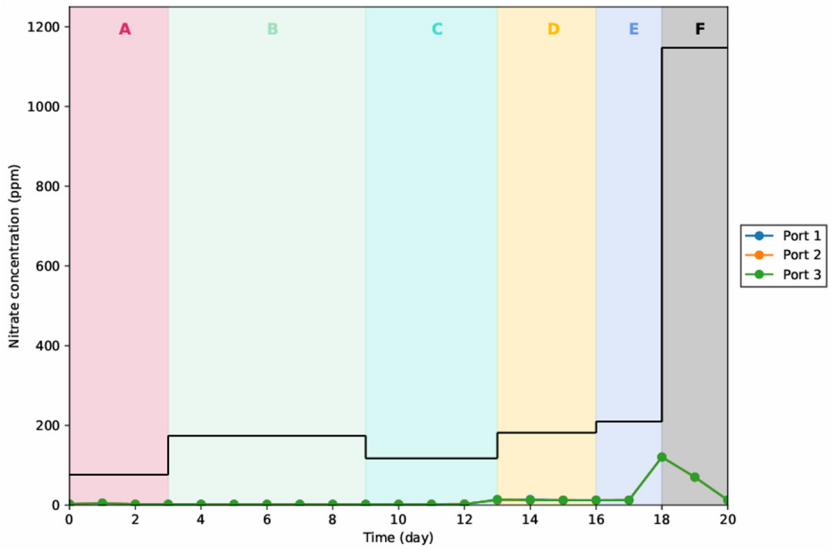

Figure 6. Run 1 effluent nitrate concentration monitoring profile measured at sample ports 1–2. The letters (A–F) at the top of the graph represent the different influent conditions mentioned in Table 3, i.e., Section A—80 ppm feed.

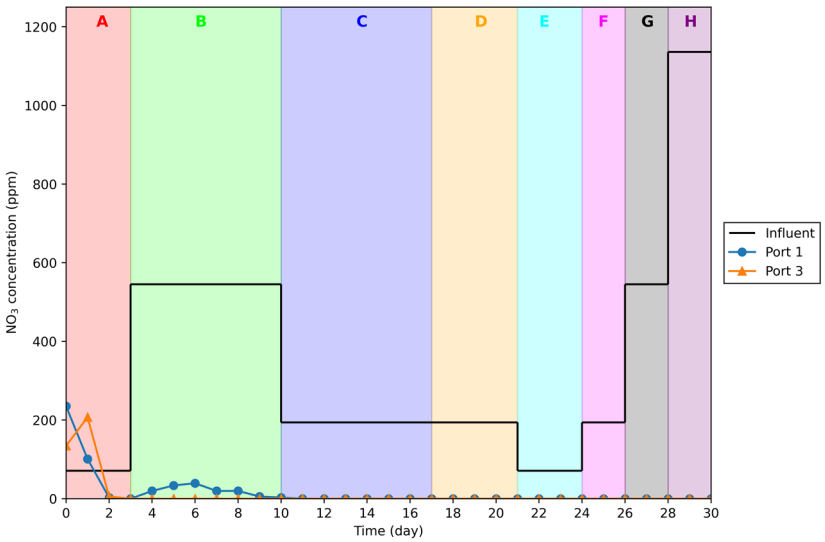

Figure 7. Run 2 effluent nitrate concentration monitoring profile measured at sample points 1 and 3. The letters (A–H) at the top of the graph represent the different influent conditions mentioned in Table 4, i.e., Section A—80 ppm feed.

In both experimental runs, nitrate concentrations were consistently degraded across all Pb(II) concentrations, though occasional spikes were observed. During the first run, a spike occurred between days 17 and 20, likely due to the increased inlet Pb(II) concentration from $Pb(NO_3)_2$. In the second run, no significant spikes were seen after day 2, with the initial spike most likely resulting from residual NO_3^- ions from previous experimental runs.

In the first run, both Pb(II) and nitrate removal were achieved, suggesting that secondary mechanisms such as sulfur-reducing bacteria, bioprecipitation, or biosorption were working in conjunction with denitrification. However, after day 17, elevated nitrate concentrations, along with slightly increased Pb(II) levels in the effluent, indicated that the bioremoval process was hindered at higher influent Pb(II) concentrations. This suggests that denitrification and secondary detoxification mechanisms were negatively impacted under these conditions.

In the second run, denitrification appeared to be the dominant detoxifying mechanism, as there were no significant spikes in either Pb(II) or nitrate concentrations throughout the run. The uniformity of Pb(II) concentrations at all sampling points in both runs supports the earlier conclusion that the reactor did not have significant dead zones, ensuring effective detoxification throughout the system.

4. Conclusions

The study described observations made during the operation of a UASB reactor under continuous anoxic conditions for the removal of Pb(II) from an aqueous environment. Nitrate and Pb(II) concentrations were monitored over two experimental runs to assess the capabilities of the microbiome when exposed to varying Pb(II) levels. A genetic study was conducted alongside these measurements to better understand the detoxification mechanisms and bacterial strains involved under continuous operation. The system demonstrated robustness, showing that with proper nutrient availability, Pb(II) bioremediation of up to 99% efficiency was achievable at concentrations as high as 2000 ppm. During the most effective run, the effluent concentration was maintained between 0–4.15 ppm.

Denitrification emerged as the dominant detoxification mechanism in both runs, although other mechanisms such as biosorption, sulfur-reducing bacteria activity, bioprecipitation, and bioremoval were also observed. Nutrient concentration played a crucial role in lead removal efficiency, with 15 g/L YE yielding significantly better results than 5 g/L YE. The precipitate recovered from the reactor—containing elemental lead, PbS, and PbO—suggests a potential route for lead recovery, adding a circular aspect to the proposed bioremediation strategy. The presence of these lead species indicates the possibility of using the precipitate as feedstock for lead smelting processes. Overall, the system shows great potential for biological lead bioremediation and recovery, offering a sustainable solution for handling lead-contaminated environments.

5. Future Research and Recommendations

Preliminary results observations indicate that this bioremediation strategy has the potential to be quite effective. However, there are some improvements that can be made to provide more insight into the robustness of the microbial community.

To begin with, the use of simulated wastewater in this study can be improved by using actual wastewater from mining waste tailings and battery effluents. Using these practical examples of effluents will give an insight into how the microbes would be able to handle wastewater that has Pb contamination as well as other heavy metals. The concentration range of industry grade effluents is also higher than the testing ranges, this would give a better measure of the bioremediation strategy's effectiveness.

The detection of Pb species in the precipitate is not enough to suggest that recovery is effective. Mass balances should be done to calculate how much Pb from the influent reports to the precipitate. Quantifying this would be necessary to elucidate how much Pb can be recovered using this process and a comparison can be made to conventional methods.

Author Contributions: Conceptualization, B.M.M., H.G.B. and E.C., methodology, B.M.M., C.C. and H.G.B., software, H.G.B.; validation, H.G.B., J.T.T., C.C., E.C. and N.H.H.; formal analysis, H.G.B., C.C., J.T.T., E.C. and N.H.H.; investigation, B.M.M. and H.G.B.; resources, H.G.B.; data curation, B.M.M. and H.G.B.; writing—original draft preparation, B.M.M., H.G.B. and E.C.; writing—review and editing, H.G.B., C.C., N.H.H., J.T.T. and E.C.; supervision, H.G.B. and E.C.; project administration, H.G.B. and E.C.; funding acquisition, H.G.B., N.H.H. and E.C. All authors have read and agreed to the published version of the manuscript.

Funding: This study was funded by National Research Foundation (NRF) of South Africa [CSRP220420402]. The work was further supported by the Austrian Federal Ministry of Education, Science and Research (BMBWF) through Austria's Agency for Education and Internationalization (OeAD) [Grant numbers: Africa UNINET P056 and P058 as well as APPEAR Project 341]. APPEAR is a program of the Austrian Development Organization.

Institutional Review Board Statement: Not applicable.

Informed Consent Statement: Not applicable.

Data Availability Statement: The raw data supporting the conclusions of this article will be made available by the authors upon request.

Acknowledgments: Open Access Funding by the University for Continuing Education Krems.

Conflicts of Interest: The authors declare no conflicts of interest. The funders had no role in the design of the study; in the collection, analyses, or interpretation of data; in the writing of the manuscript; or in the decision to publish the results.

Appendix A

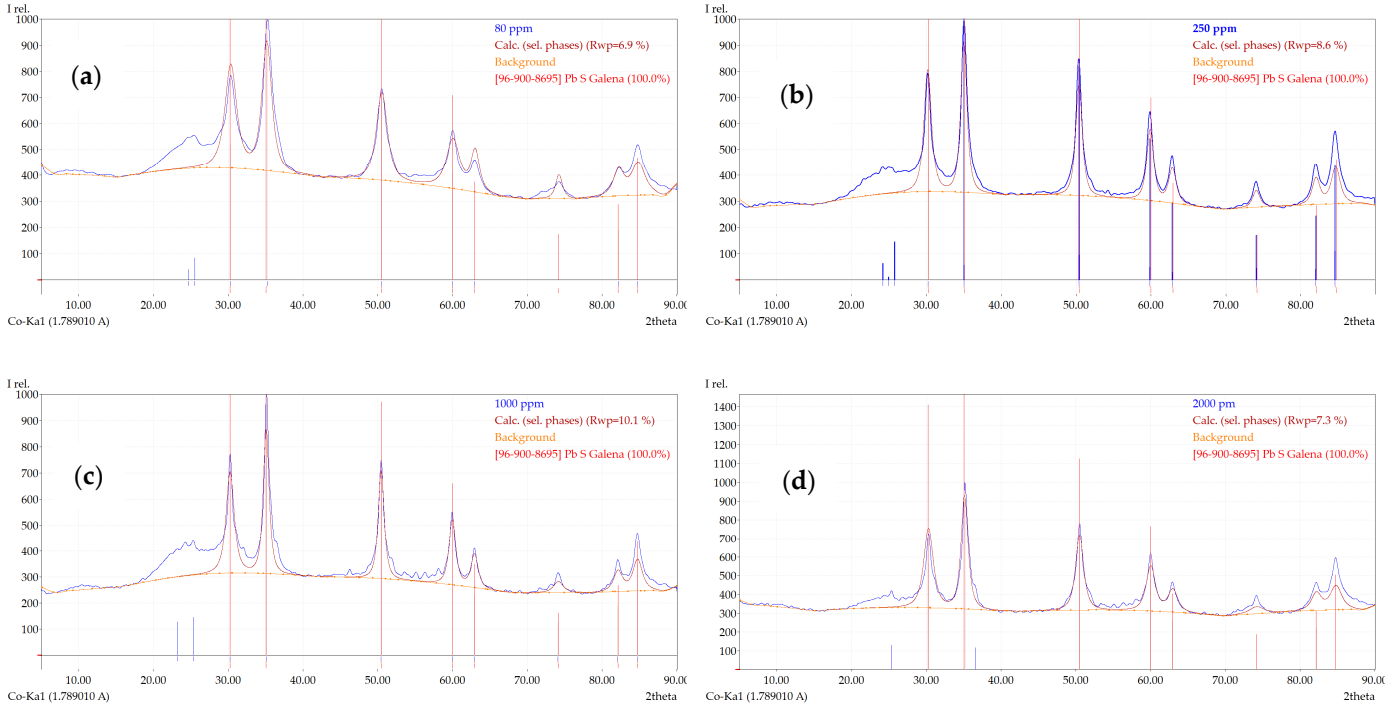

Figure A1. XRD profiles of the reactor precipitate taken at (**a**) 80 ppm feed concentration, (**b**) 250 ppm (**c**) 1000 ppm, and (**d**) 2000 ppm concentration feed. All show 100% PbS in the precipitate.

References

1. Meyer, P.A.; Brown, M.J.; Falk, H. Global approach to reducing lead exposure and poisoning. *Mutat. Res.* **2008**, *659*, 166–175. [CrossRef]
2. Chatterjee, S.; Mukherjee, A.; Sarker, A.; Pranab, R. Bioremediation of lead by lead resistant microorganisms, isolated from industrial sample. *Adv. Biosci. Biotechnol.* **2012**, *3*, 290–295. [CrossRef]

3. Naik, M.M.; Dubey, S.K. Lead Resistant Bacteria: Lead Resistance Mechanisms, Their Applications in Lead Bioremediation and Biomonitoring. *Ecotoxicol. Environ. Saf.* **2013**, *98*, 1–7. [CrossRef]
4. Tchounwou, P.B.; Yedjou, C.G.; Patlolla, A.K.; Sutton, D.J. Heavy Metals Toxicity and the Environment. *Mol. Clin. Environ. Toxicol. Experentia Supplentum* **2012**, *101*, 134–164.
5. Supanopas, P.; Sretarugsa, P.; Kruatrachue, M.; Pokethitiyook, P.; Upatham, S. Acute and Subchronic Toxicity of Lead To the Spotted Babylon, Babylonia Areolata (Neogastropoda, Buccinidae). *J. Shellfish Res.* **2005**, *24*, 91–98.
6. Papp, A.; Pecze, L.; Szabó, A.; Vezér, T. Effects on the central and peripheral nervous activity in rats elicited by acute administration of lead, mercury and manganese, and their combinations. *J. Appl. Toxicol. JAT* **2006**, *26*, 374–380. [CrossRef]
7. Eisler, R. Lead hazards to fish, wildlife and inverterbrates: A synoptic review. In *Report 14, Biological Report 85(1.14)*; U.S. Department of the Interior, Fish and Wildlife Service: Laurel, MD, USA, 1988.
8. Brink, H.G.; Lategan, M.; Naude, K.; Chirwa, E.M.N. Lead Removal Using Industrially Sourced Consortia: Influence of Lead and Glucose Concentrations. *Chem. Eng. Trans.* **2017**, *57*, 409–414.
9. Arbabi, M.; Hemati, S.; Amiri, M. Removal of Lead ions from industrial wastewater: A review of removal methods. *Int. J. Epidemiol. Res.* **2015**, *2*, 105–109.
10. Mamba, B.; Rietveld, L.; Verberk, J.S.A. Drinking Water Standards under the microscope. *Water Wheel* **2008**, *7*, 24–27.
11. UNEP. *Final Review of Scientific Information on Lead*; United Nations: New York, NY, USA, 2010.
12. Hama Aziz, K.; Mustafa, F.S.; Omer, K.M.; Hama, S.; Hamarawf, R.F.; Rahman, K.O. Heavy metal pollution in the aquatic environment: Efficient and low-cost removal approaches to eliminate their toxicity: A review. *RSC Adv.* **2023**, *13*, 17595–17610. [CrossRef]
13. CDFA. Lead Toxicity and its Effects on Animals and Animal Products. [Website document] 2016 July 2016. Available online: https://www.cdfa.ca.gov/ahfss/Animal_Health/pdfs/leadtoxicity.pdf (accessed on 18 June 2024).
14. Sharma, A.; Kaur, M.; Katnoria, J.K.; Nagpal, A.K. Heavy Metal Pollution: A Global Pollutant of Rising Concern. In *Toxicity and Waste Management Using Bioremediation*; Rathoure, A.K., Dhatwalia, V.K., Eds.; Engineering Science Reference: Hershey, PA, USA, 2016; pp. 1–26.
15. Oulhote, Y.; LeTertre, A.; Etchevers, A.; Le Bot, B.; Lucas, J.P.; Mandin, C.; Le Strat, Y.; Lanphear, B.; Glorennec, P. Implications of different residential lead standards on children's blood lead levels in France: Predictions based on a national cross-sectional survey. *Int. J. Hyg. Environ. Health* **2013**, *216*, 743–750. [CrossRef]
16. Xiang, H.; Min, X.; Tang, C.-J.; Sillanpää, M.; Zhao, F. Recent advances in membrane filtration for heavy metal removal from wastewater: A mini review. *J. Water Process Eng.* **2022**, *49*, 103023. [CrossRef]
17. Brink, H.G.; Hörstmann, C.; Peens, J. Microbial Pb(II)-precipitation: The influence of oxygen on Pb(II)-removal from aqueous environment and the resulting precipitate identity. *Int. J. Environ. Sci. Technol.* **2019**, *17*, 409–420. [CrossRef]
18. Pohl, A. Removal of Heavy Metal Ions from Water and Wastewaters by Sulfur-Containing Precipitation Agents. *Water Air Soil Pollut.* **2020**, *231*, 503. [CrossRef]
19. Fu, F.; Wang, Q. Removal of Heavy Metal Ions from Wastewaters: A Review. *J. Environ. Manag.* **2011**, *92*, 407–418. [CrossRef]
20. Ngwenya, N.; Chirwa, E.M.N. Single and binary component sorption of the fission products Sr^{2+}, Cs^{+} and Co^{2+} from aqueous solutions onto sulphate reducing bacteria. *Miner. Eng.* **2010**, *23*, 463–470. [CrossRef]
21. Bosso, L.; Scelza, R.; Varlese, R.; Meca, G.; Testa, A.; Rao, M.A.; Cristinzio, G. Assessing the effectiveness of Byssochlamys nivea and Scopulariopsis brumptii in pentachlorophenol removal and biological control of two Phytophthora species. *Fungal Biol.* **2016**, *120*, 645–653. [CrossRef]
22. Ayangbenro, A.S.; Olanrewaju, O.S.; Babalola, O.O. Sulfate-reducing bacteria as an effective tool for sustainable acid mine bioremediation. *Front. Microbiol.* **2018**, *9*, 1986. [CrossRef]
23. Singh, S.; Kang, S.H.; Mulchandani, A.; Chen, W. Bioremediation: Environmental clean-up through pathway engineering. *Curr. Opin. Biotechnol.* **2008**, *19*, 437–444. [CrossRef]
24. Philp, J.; Bamforth, S.; Singleton, I.; Atlas, R. Environmental Pollution and Restoration: A Role for Bioremediation. In *Bioremediation: Applied Microbial Solutions for Real-World Environmental Cleanup*; Philp, J., Atlas, R., Eds.; American Society for Microbiology: Washington, DC, USA, 2005; pp. 1–24.
25. Rathoure, A.K. Heavy Metal Pollution and its Management: Bioremediation of Heavy Metals. In *Toxicity and Waste Management Using Bioremediation*; Rathoure, A.K., Dhatwalia, V.K., Eds.; Engineering Science Reference: Hershey, PA, USA, 2016; pp. 27–50.
26. Adeniji, A. *Bioremediation of Arsenic, Chromium, Lead and Mercury*; EPA Report: Washington, DC, USA, 2004.
27. Lakhani, S.; Acharya, D.; Sakariya, R.; Sharma, D.; Patel, P.; Shah, M.; Prajapati, M. A comprehensive study of bioremediation for pharmaceutical wastewater treatment. *Clean. Chem. Eng.* **2022**, *4*, 100073. [CrossRef]
28. Narayanan, C.M.; Narayan, V. Biological Wastewater Treatment and Bioreactor Design: A Review. *Sustain. Environ. Res.* **2019**, *29*, 33. [CrossRef]
29. Ali, A.S.; Bayih, A.A.; Gari, S.R. Meta-analysis of public health risks of lead accumulation in wastewater, irrigated soil, and crops nexus. *Front. Public Health* **2022**, *10*, 977721. [CrossRef]
30. Rambabu, K.; Banat, F.; Pham, Q.M.; Ho, S.-H.; Ren, N.-Q.; Show, P.L. Biological remediation of acid mine drainage: Review of past trends and current outlook. *Environ. Sci. Ecotechnol.* **2020**, *2*, 100024. [CrossRef]
31. IWA Publishing. *Up Flow—Anaerobic Sludge Blanket Reactor (UASB)*; IWA Publishing: London, UK, 2024. Available online: https://www.iwapublishing.com/news/flow-anaerobic-sludge-blanket-reactor-uasb (accessed on 31 October 2024).

32. Macchi, G.; Pagano, M.; Santori, M.; Tiravanti, G. Battery industry wastewater: Pb removal and produced sludge. *Water Res.* **1993**, *27*, 1511–1518. [CrossRef]
33. Chimhundi, J.; Hörstmann, C.; Chirwa, E.M.N.; Brink, H. Microbial Removal of Pb(II) using an Upflow Anaerobic Sludge Blanket (UASB) Reactor. *Catalysts* **2021**, *11*, 512. [CrossRef]
34. Tendendzai, J.T.; Chirwa, E.M.N.; Brink, H.G. *Enterococcus* spp. Cell-Free Extract: An Abiotic Route for Synthesis of Selenium Nanoparticles (SeNPs), Their Characterisation and Inhibition of *Escherichia coli*. *Nanomaterials* **2022**, *12*, 658. [CrossRef]
35. Rodríguez-Carvajal, J. Recent advances in magnetic structure determination by neutron powder diffraction. *Phys. B Condens. Matter* **1993**, *192*, 55–69. [CrossRef]
36. Gupta, J.; Hassan, P.A.; Barick, K.C. 12—Defects in nanomaterials for visible light photocatalysis. In *Micro and Nano Technologies*; Nayak, A.K., Sahu, N.K., Eds.; Elsevier: Amsterdam, The Netherlands, 2022; pp. 319–350.
37. QIAGEN, 2013. DNeasy 96 PowerSoil Pro Kit. Available online: https://www.qiagen.com/pl/products/discovery-and-translational-research/dna-rna-purification/dna-purification/microbial-dna/dneasy-96-powersoil-pro-kit (accessed on 23 August 2024).
38. ZymoBIOMICS. ZymoBIOMICS DNA Miniprep Kit. 2024. Available online: https://zymoresearch.eu/collections/zymobiomics-dna-kits/products/zymobiomics-dna-miniprep-kit (accessed on 11 November 2024).
39. Ponti, G.; Maccaferri, M.; Manfredini, M.; Kaleci, S.; Mandrioli, M.; Pellacani, G.; Ozben, T.; Depenni, R.; Bianchi, G.; Pirola, G.M.; et al. The value of fluorimetry (Qubit) and spectrophotometry (NanoDrop) in the quantification of cell-free DNA (cfDNA) in malignant melanoma and prostate cancer patients. *Clin. Chim. Acta* **2018**, *479*, 14–19. [CrossRef]
40. Barril, P.; Nates, S. Introduction to agarose and polyacrylamide gel electrophoresis matrices with respect to their detection sensitivities. In *Gel Eectrophoresis-Principles and Basics*; Magdeldin, S., Ed.; InTech: Rijeka, Croatia, 2012; pp. 3–14.
41. Armstrong, J.A.; Schulz, J.R. Agarose gel electrophoresis. *Curr. Protoc. Essent. Lab. Tech.* **2015**, *10*, 7.2.1–7.2.22. [CrossRef]
42. Buetas, E.; Jordán-López, M.; López-Roldán, A.; D'Auria, G.; Martínez-Priego, L.; De Marco, G.; Carda-Diéguez, M.; Mira, A. Full-length 16S rRNA gene sequencing by PacBio improves taxonomic resolution in human microbiome samples. *BMC Genom.* **2024**, *25*, 310. [CrossRef]
43. Preparing Multiplexed Amplicon Libraries Using PacBio Barcoded M13 Primers and SMRTbell® Prep Kit 3.0. 2023. Available online: https://crtp.ccr.cancer.gov/wp-content/uploads/2023/10/Procedure-checklist-Preparing-multiplexed-amplicon-libraries-using-SMRTbell-prep-kit-3.0.pdf (accessed on 11 October 2024).
44. Manzini, B.M.; Cilliers, C.; Brink, H.G.; Chirwa, E.M.N. Continuous Microbial Pb Removal by an Industrially Obtained Consortium Using an Upflow Anaerobic Sludge Blanket Reactor. *Chem. Eng. Trans.* **2024**, *110*, 193–198.
45. Sevak, P.I.; Pushkar, B.K.; Kapadne, P.N. Lead pollution and bacterial bioremediation: A review. *Environ. Chem. Lett.* **2021**, *19*, 4463–4488. [CrossRef]
46. *pH in Drinking Water*; World Health Organization: Geneva, Switzerland, 2007.
47. Swart, M. Rand Water: Johannesburg, South Africa; 2024. Available online: https://randwater.co.za/media/forums/presentations/South%20African%20National%20StandardDrinking%20Water%20Quality%20SANS%20241%20%202024).pdf (accessed on 16 September 2024).
48. Cilliers, C.; Chirwa, E.M.; Brink, H.G. Insight into the metabolic profiles of pb(Ii) removing microorganisms. *Molecules* **2021**, *26*, 4008. [CrossRef]
49. Tanes, C.; Tu, V.; Scott, D.; Bittinger, K. Unassigning bacterial species for microbiome studies. *ASM J.* **2024**, *9*, e00515-24. [CrossRef]
50. Richardson, J.; Dancy, B.C.R.; Horton, C.L.; Lee, Y.S.; Madejczyk, M.S.; Xu, Z.Z.; Ackermann, G.; Humphrey, G.; Palacios, G.; Knight, R.; et al. Exposure to toxic metals triggers unique responses from the rat gut microbiota. *Sci. Rep.* **2018**, *8*, 6578. [CrossRef]
51. Das, P.; Babaei, P.; Nielsen, J. Metagenomic analysis of microbe-mediated vitamin metabolism in the human gut microbiome. *BMC Genom.* **2019**, *20*, 208. [CrossRef]
52. Gomilla, M.; Peña, A.; Mulet, M.; Lalucat, J.; García-Valdés, E. Phylogenomics and systematics in Pseudomonas. *Front. Microbiol.* **2015**, *6*, 1–13. [CrossRef]
53. Dandachi, I.; Anani, H.; Hadjadj, L.; Brahimi, S.; Lagier, J.C.; Daoud, Z.; Rolain, J.M. Genome analysis of Lachnoclostridium phocaeense isolated from a patient after kidney transplantation in Marseille. *New Microbes New Infect.* **2021**, *41*, 100863. [CrossRef]
54. Hemmat-Jou, M.H.; Safari-Sinegani, A.A.; Mirzaie-Asl, A.; Tahmourespour, A. Analysis of microbial communities in heavy metals-contaminated soils using the metagenomic approach. *Ecotoxicology* **2018**, *27*, 1281–1291. [CrossRef]
55. Neveling, O.; Ncube, T.M.C.; Ngxongo, Z.P.; Chirwa, E.M.N.; Brink, H.G. Microbial Precipitation of Pb (II) with Wild Strains of Paraclostridium bifermentans and Klebsiella pneumoniae Isolated from an Industrially Obtained Microbial Consortium. *Int. J. Mol. Sci.* **2022**, *23*, 12255. [CrossRef]
56. Alexandrino, M.; Costa, R.; Canario, A.V.; Costa, M.C. Clostridia Initiate Heavy Metal Bioremoval in Mixed Sul fi dogenic Cultures. *Environ. Sci. Technol.* **2014**, *48*, 3378–3385. [CrossRef]
57. De Niederhäusern, S.; Bondi, M.; Anacarso, I.; Iseppi, R.; Sabia, C.; Bitonte, F.; Messi, P. Antibiotics and heavy metals resistance and other biological characters in enterococci isolated from surface water of Monte Cotugno Lake (Italy). *J. Environ. Sci. Health Part A* **2013**, *48*, 939–946. [CrossRef]
58. Kerkhof, P.J.; Van den Abeele, A.M.; Strubbe, B.; Vogelaers, D.; Vandamme, P.; Houf, K. Diagnostic approach for detection and identification of emerging enteric pathogens revisited: The (Ali)arcobacter lanthieri case. *New Microbes New Infect.* **2021**, *39*, 100829. [CrossRef]

59. Çelik, C.; Pınar, O.; Sipahi, N. The Prevalence of Aliarcobacter Species in the Fecal Microbiota of Farm Animals and Potential Effective Agents for Their Treatment: A Review of the Past Decade. *Microorganisms* **2022**, *10*, 2430. [CrossRef]
60. Parikh, R.; Singh, S.; Prasad, B.L.; Patole, M.S.; Sastry, M.; Shouche, Y.S. Extracellular synthesis of crystalline silver nanoparticles and molecular evidence of silver resistance from *Morganella* sp.: Towards understanding biochemical synthesis mechanism. *Chembiochem* **2008**, *9*, 1415–1422. [CrossRef]
61. Yasawong, M.; Wongchitrat, P.; Isarankura-Na-Ayudhya, C.; Isarankura-Na-Ayudhya, P.; Na Nakorn, P. Draft genome sequence data of heavy metal-resistant Morganella morganii WA01/MUTU, a silver nanoparticle (AgNP) synthesising bacterium. *Data in Brief* **2024**, *52*, 109873. [CrossRef]
62. Arat, S.; Bullerjahn, G.S.; Laubenbacher, R. A Network Biology Approach to Denitrification in Pseudomonas aeruginosa. *PLoS ONE* **2015**, *10*, e0118235. [CrossRef]
63. Fadel, M.; Hassanein, N.; Elshafai, M.; Mostafa, A.; Ahmed, M.; Khater, H. Biosorption of manganese from groundwater by biomass of Saccharomyces cerevisiae. *HBRC J.* **2017**, *13*, 106–113. [CrossRef]
64. Velez, J.M.B.; Martínez, J.G.; Ospina, J.T.; Agudelo, S.O. Bioremediation potential of Pseudomonas genus isolates from residual water, capable of tolerating lead through mechanisms of exopolysaccharide production and biosorption. *Biotechnol. Rep.* **2021**, *32*, e00685. [CrossRef]
65. Liu, W.; Feng, H.; Zheng, S.; Xu, S.; Massey, I.Y.; Zhang, C.; Wang, X.; Yang, F. Pb Toxicity on Gut Physiology and Microbiota. *Front. Physiol.* **2021**, *10*, 574913. [CrossRef]
66. Feng, Y.; Feng, J.; Shu, Q.L. Isolation and characterization of heterotrophic nitrifying and aerobic denitrifying Klebsiella pneumoniae and Klebsiella variicola strains from various environments. *J. Appl. Microbiol.* **2018**, *2*, 1195–1211. [CrossRef] [PubMed]
67. Mohan, A.K.; Chiplunkar, S.; Kamath, S.; Goveas, L.; Rao, C.V.; Shiny, M.B. Heavy Metal Tolerance of Klebsiella pneumoniae Kpn555 Isolated from Coffee Pulp Waste. *Borneo J. Resour. Sci. Technol.* **2019**, *9*, 101–106.
68. Fang, H.; Oberoi, A.S.; He, Z.; Khanal, S.K.; Lu, H. Ciprofloxacin-degrading Paraclostridium sp. isolated from Sulfate-reducing bacteria enriched sludge: Optimization and mechanism. *Water Res.* **2021**, *191*, 116808. [CrossRef] [PubMed]
69. Heylen, K.; Vanparys, B.; Wittebolle, L.; Verstraete, W.; Boon, N.; De Vos, P. Cultivation of Denitrifying Bacteria: Optimization of Isolation Conditions and Diversity Study. *Appl. Environ. Biol.* **2006**, *72*, 2637–2643. [CrossRef]
70. Said, M.S.; Tirthani, E.; Lesho, E. *Enterococcus Infections*; StatPearls: Treasure Island, FL, USA, 2022; pp. 1–14.
71. Topcu, A.; Bulat, T. Removal of Cadmium and Lead from Aqueous Solution by Enterococcus faecium Strains. *J. Food Sci.* **2010**, *75*, T13–T17. [CrossRef]
72. Huang, J.; Huang, Z.-L.; Zhou, J.; Li, C.-Z.; Yang, Z.-H.; Ruan, M.; Li, H.; Zhang, X.; Wu, Z.-J.; Qin, X.-L.; et al. Enhancement of heavy metals removal by microbial flocculant produced by Paenibacillus polymyxa combined with an insufficient hydroxide precipitation. *Chem. Eng. J.* **2019**, *374*, 880–894. [CrossRef]
73. Sáez-Nieto, J.A.; Medina, M.J.; Carrasco, G.; Garrido, N.; Fernandez-Torres, M.A.; Villalón, P.; Valdezate, S. Paenibacillus spp. isolated from human and environmental samples in Spain: Detection of 11 new species. *New Microbes New Infect.* **2017**, *19*, 19–27. [CrossRef]
74. Bridges, C.; Gage, D. Development and application of aerobic, chemically defined media for *Dysgonomonas*. *Anaerobe* **2021**, *67*, 102302. [CrossRef]
75. Gao, X.; Wei, J.; Hao, T.; Yang, T.; Han, X.; Li, M.; Li, X.; Xiong, D.; Zhang, X. *Dysgonomonas mossii* Strain Shenzhen WH 0221, a New Member of the Genus Dysgonomonas Isolated from the Blood of a Patient with Diabetic Nephropathy, Exhibits Multiple Antibiotic Resistance. *Microbiol. Spectr.* **2022**, *10*, e02381-21. [CrossRef]
76. Shakoori, A.; Muneer, B. Copper-resistant bacteria from industrial effluents and their role in remediation of heavy metals in wastewater. *Folia Microbiol.* **2002**, *47*, 43–50. [CrossRef]
77. Brunswick, J.; Spiro, J.; Wisniewski, P. Vagococcus: An under-recognized and emerging cause of antibiotic-resistant infection. *Idcases* **2024**, *36*, e01995. [CrossRef] [PubMed]
78. Yan, Y.; Twible, L.E.; Liu, F.Y.L.; Arrey, J.L.S.; Colenbrander Nelson, T.E.; Warren, L.A. Cascading sulfur cycling in simulated oil sands pit lake water cap mesocosms transitioning from oxic to euxinic conditions. *Sci. Total Environ.* **2024**, *950*, 175272. [CrossRef] [PubMed]
79. Rickard, D. Chapter 14—Sedimentary Sulfides. In *Developments in Sedimentology*; Rickard, D., Ed.; Elsevier: Amsterdam, The Netherlands, 2012; pp. 543–604.